THE JOURNAL OF BIOLOGICAL CHEMISTRY VOL. 290, NO. 24, pp. 15052–15065, June 12, 2015

Metabotropic Glutamate Receptors

MODULATORS OF CONTEXT-DEPENDENT FEEDING BEHAVIOUR IN C. ELEGANS

Received for publication, August 22, 2014, and in revised form, April 9, 2015 Published, JBC Papers in Press, April 13, 2015, DOI 10.1074/jbc.M114.606608

James Dillon[‡1], Christopher J. Franks[‡2], Caitriona Murray[§2], Richard J. Edwards[¶], Fernando Calahorro[‡3], Takeshi Ishihara[‖], Isao Katsura[**], Lindy Holden-Dye[‡], and Vincent O'Connor[‡4]

*From the [‡]Centre for Biological Sciences, University of Southampton, University Road, Southampton, SO17 1BJ, United Kingdom, the [§]Ramaciotti Centre for Genomics and [¶]School of Biotechnology and Biomolecular Sciences, University of New South Wales, Kensington, New South Wales 2052, Australia, the [‖]Department of Biology, Graduate School of Science, Kyushu University, 6-10-1, Hakozaki, Higashi-ku, Fukuoka 812-8581, Japan, and the **National Institute of Genetics, Yata 1111, Mishima, Shizuoka-ken, 411-8540, Japan*

Background: *C. elegans* encodes three metabotropic glutamate receptors: *mgl-1*, *mgl-2*, and *mgl-3*.
Results: *mgl-1* and *mgl-3*, but not *mgl-2*, modulate activity in the neural circuit underlying feeding behavior.
Conclusion: *mgl-1* is the major contributor to the inhibitory tone of the feeding circuit and context-dependent feeding behavior.
Significance: *C. elegans* provides a model for systems-level understanding of metabotropic glutamate receptors.

Glutamatergic neurotransmission is evolutionarily conserved across animal phyla. A major class of glutamate receptors consists of the metabotropic glutamate receptors (mGluRs). In *C. elegans*, three mGluR genes, *mgl-1*, *mgl-2*, and *mgl-3*, are organized into three subgroups, similar to their mammalian counterparts. Cellular reporters identified expression of the *mgl*s in the nervous system of *C. elegans* and overlapping expression in the pharyngeal microcircuit that controls pharyngeal muscle activity and feeding behavior. The overlapping expression of *mgl*s within this circuit allowed the investigation of receptor signaling *per se* and in the context of receptor interactions within a neural network that regulates feeding. We utilized the pharmacological manipulation of neuronally regulated pumping of the pharyngeal muscle in the wild-type and mutants to investigate MGL function. This defined a net *mgl-1*-dependent inhibition of pharyngeal pumping that is modulated by *mgl-3* excitation. Optogenetic activation of the pharyngeal glutamatergic inputs combined with electrophysiological recordings from the isolated pharyngeal preparations provided further evidence for a presynaptic *mgl-1*-dependent regulation of pharyngeal activity. Analysis of *mgl-1*, *mgl-2*, and *mgl-3* mutant feeding behavior in the intact organism after acute food removal identified a significant role for *mgl-1* in the regulation of an adaptive feeding response. Our data describe the molecular and cellular organization of *mgl-1*, *mgl-2*, and *mgl-3*. Pharmacological analysis identified that, in these paradigms, *mgl-1* and *mgl-3*, but not *mgl-2*, can modulate the pharyngeal microcircuit. Behavioral analysis identified *mgl-1* as a significant determinant of the glutamate-dependent modulation of feeding, further highlighting the significance of mGluRs in complex *C. elegans* behavior.

In mammals, glutamate signals broadly via two classes of receptors: the ionotropic glutamate receptors and metabotropic glutamate receptors (mGluRs)[5] (1, 2). mGluRs are G protein-coupled receptors and perform an important neuromodulatory role in glutamatergic transmission within the mammalian nervous system (3, 4). The importance of this class of receptors is highlighted by their involvement in a number of different neurological conditions, including anxiety, autism, and schizophrenia (5, 6). Interestingly, it has been proposed that each of these conditions involves a loss of the balance between cellular inhibition and excitation within the context of discrete microcircuits (7–9). As neuromodulators, mGluRs represent attractive targets to manipulate the excitatory-inhibitory balance and alleviate the behavioral dysfunction and sensory deficits associated with these conditions (6, 10). Therefore, an understanding of mGluR contribution to the balance of activity within a microcircuit is potentially beneficial within the broader context of neurological disorders in which this imbalance has been suggested as an underlying cause.

Both the ionotropic glutamate receptor and mGluR classes of receptors are conserved within the genome of the model organism *Caenorhabditis elegans*. In *C. elegans*, the ionotropic glutamate receptor subfamily is well characterized and encompasses mammalian NMDA and AMPA-like receptors together with an invertebrate-specific subgroup of glutamate-gated chloride ion channels (11). The *C. elegans* genome encodes at least three mGluRs, designated *mgl-1*, *mgl-2*, and *mgl-3*. Although the experimental tractability of *C. elegans* has provided insight into the molecular, cellular, and functional organization of the ionotropic glutamate receptor family (11), com-

[1] Supported by a Biotechnology and Biological Sciences Research Council (BBSRC) Committee Studentship Grant BB/F009208/1 and the Gerald Kerkut Charitable Trust. To whom correspondence may be addressed: Centre for Biological Sciences, University of Southampton, University Rd., Southampton SO17 1BJ, Hants., UK. E-mail: jcd@soton.ac.uk.
[2] Supported by the BBSRC.
[3] Supported by Grant Fellowship EF0002 from Consejería de Salud, Junta de Andalucía, Spain.
[4] To whom correspondence may be addressed: Centre for Biological Sciences, University of Southampton, University Rd., Southampton SO17 1BJ, Hants., UK. E-mail: voconno@soton.ac.uk.

[5] The abbreviations used are: mGluR, metabotropic glutamate receptor; RACE, rapid amplification of cDNA ends; SL, splice leader; EPG, electropharyngeogram; (±)trans-ACPD, (±)-1-aminocyclopentane-trans-1,3-dicarboxylic acid; LCCG-I, (2S,1′S,2′S)-2-(carboxycyclopropyl)glycine.

paratively less is known about the function of the MGL class of receptors in *C. elegans*. The identification of mGluRs in invertebrates that are closely related to specific vertebrate mGluR subtypes suggests that this class of receptors may play a similarly important role in signaling and adaptive behavior within simpler organisms (12–15).

C. elegans displays a number of rhythmic behaviors that undergo adaptation and are modulated by the activity of simple microcircuits that integrate sensory information from both the external and internal environment of the worm. A key sensory cue that governs the pattern of activity within these microcircuits is food (16, 17). Indeed, dopaminergic, cholinergic, and 5-HT signaling via G protein-coupled receptors has been shown previously to contribute to a number of food-dependent behaviors that encompass changes in patterns of locomotory subbehaviors and pharyngeal function (18–20). Therefore, the presentation and removal of a sensory cue, such as food, represents two very distinct contexts that change the behavior of the worms by separate signaling pathways. In *C. elegans*, context-dependent signaling has been resolved at the level of neurons expressed within circuits that are responsible for either the detection of sensory cues or the integration of sensory signals with motor coordination. For example, the glutamatergic circuitry involved in chemotaxis toward an attractant contains both OFF-sensing neurons, which are active in the absence of an attractant, and ON-sensing neurons, which are active in the presence of an attractant. OFF and ON situations represent distinct contextual states, and the coordinated signaling between OFF-sensing and ON-sensing neurons provides a mechanism by which *C. elegans* can initiate adaptive changes in behavior in response to contextual changes such as the presentation and removal of a sensory cue (21). *C. elegans* feeding behavior has been shown previously to change upon the presentation and removal of food (20, 22), highlighting that circuits contributing to the activity of the pharynx are subject to context-dependent signaling. The observation that glutamate signaling can activate circuits to mimic feeding behavior in the OFF-food state implicates a role for this neurotransmitter pathway in the context-dependent modulation of the pharyngeal nervous system (46). Glutamatergic signaling and specific receptors therein may therefore contribute to the signaling pathways underlying context-dependent changes in *C. elegans* feeding behavior.

Here we describe three metabotropic glutamate receptors that have a widespread expression in the nervous system of *C. elegans*. The *mgls* appear to be differentially expressed exclusively in the nervous system of *C. elegans*. *mgl-1*, *mgl-2*, and *mgl-3* expression in the pharyngeal nervous system suggests their involvement in the modulation of pharyngeal network activity. Electrophysiological recordings on a semi-intact preparation of the *C. elegans* pharynx, combined with the use of mGluR agonists and worms with putative null mutations identified that, under these experimental conditions, both *mgl-1* and *mgl-3*, but not *mgl-2*, can modulate the activity of the pharyngeal circuit. Experiments performed on intact animals suggest that, of the three receptors, *mgl-1* makes a significant contribution to changes in feeding behavior upon acute food removal and to the context-dependent modulation of *C. elegans* feeding behavior. Overall, the results reveal a role for glutamate neurotransmission and MGL receptor signaling in context-dependent feeding behaviors.

Experimental Procedures

Culturing of C. elegans

C. elegans strains were cultured under standard conditions (23). Wild-type Bristol N2 and *eat-4(ky5)* was obtained from the *Caenorhabditis* Genetics Centre. The strain *pha-1(e2123)* was obtained from R. Schnabel. The putative *mgl* knockout strains *mgl-1(tm1811)*, *mgl-2(tm0355)*, and *mgl-3(tm1766)* were obtained from the National Bioresources Project (Tokyo women's Medical University, Tokyo). The *mgl* GFP reporter strain *utIs35[mgl-1::GFP]* is a mgl-1::GFP gene fusion under the *mgl-1* promoter (as described in unpublished communication (47). The *mgl* mutant strains were outcrossed at least three times.

Molecular Phylogeny of MGL Proteins

Protein sequences for 77 metazoans with sequenced genomes were downloaded from Ensembl (version 61, March 2, 2011) (24). In addition, *Brugia malayi* proteins were downloaded from Wormbase (February 13, 2011) (25). Homologues of *C. elegans* MGL-2 (F45H11.4.2) were identified from these proteomes using BLAST (26), and the protein family was constructed with HAQESAC (27). Protein alignments were performed with MAFFT (28) using default settings. Minimum evolution molecular phylogenies were constructed using FastTree (29) with 1000 bootstrap replicates.

RACE, SL-1, and Predictive PCR Analysis

Rapid Amplification of cDNA Ends (RACE) Amplifications—Total RNA was extracted from mixed-stage Bristol N2 animals using a TRIzol® (Invitrogen) extraction method. Both reverse-transcribed mRNA and a *C. elegans* cDNA library (Origene) were used as templates for the various characterization techniques used and outlined below. All 5′-RACE products analyzed in this study were derived from two rounds of amplification using a 5′-RACE primer in the first reaction and a nested 5′-RACE primer in the second reaction, as indicated below. In contrast, all analyzed 3′-RACE products were generated using a single amplification with a 3′-RACE primer. For these experiments, 1 μg of total RNA was used to perform first-strand cDNA synthesis and incorporate either the 5′- or 3′-RACE adaptor sequence as described by the manufacturer (SMART RACE cDNA amplification kit, Clontech). The RACE adaptor-fused first-strand cDNA was used directly as the template for RACE PCR. RACE primers were designed using the sequence information available at the time. The sequences of primers used were as follows: *mgl-1* 5′-RACE (5′-GATGGCGAGCTCTCGTCATCTGTCATCCTC-3′), *mgl-1* 5′-nested RACE (5′-GTCATTGTTTCTATCCCACGACTCTGATGCAAGC-3′), *mgl-1* 3′-RACE (5′-CTCCGCCTGGGTCAACGGCATCAAGGTGC-3′), *mgl-2* 5′-RACE (5′-CGATGCTGTTCGTGTGACTCCTCCACCCATAC-3′), *mgl-2* 5′-nested RACE (5′-GTCGGATAAGTCTGGAGTGGTGGCGGAG-3′), *mgl-2* 3′-RACE (5′-GTCGGAGTTGGTTTGATGCGGGATTGGC-

CGGATG-3′), *mgl-3* 5′-RACE (5′-GAACCGGAGGAATTGGCACGAAAAATGAAGAG-3′), *mgl-3* 5′-nested RACE (5′-CGGCTCCTGTTGAACTGTAGCTGACTTGAGG-3′), and *mgl-3* 3′-RACE (5′-GAATGGTGACGGAATCGGACGATATGATGTCTTC-3′).

C-terminal Domain Amplification

Mixed-stage cDNA was used as a template in reactions designed to amplify the sequences encoding the entire intracellular C-terminal domain of the receptors. This was done with primers encoding the 5′ (5′-CT) end of this domain and the 3′ end (3′-CT) encoding the last eight to ten amino acids preceding the predicted stop codon: *mgl-1* 5′-CT (5′-GAAAAACACAAAAACGTCCGAAAG-3′), *mgl-1* 3′-CT (5′-TCATAAGAAAGTATCGTGAGC-3′), *mgl-2* 5′-CT (5′-CATCCTGAGAAGAATATCAGA-3′), *mgl-2* 3′-CT (5′-TCAAAAGATTTGCTTGAAATC-3′), *mgl-3* 5′-CT (5′-CAACCATACAAAAATGTGAGG-3′), and *mgl-3* 3′-CT (5′-TCAAAGAAAAGTGGAATTAGTGTC-3′).

Splice Leader (SL) Analysis

SL primers were designed according to the published sequences for SL-1 (5′-GGTTTAATTACCCAAGTTTGAG-3′) and SL-2 (5′-GGTTTTAACCCAGTTACTCAAG-3′). These were combined in a standard PCR reaction with *mgl-1* 5′-RACE and *mgl-3* 5′-nested RACE as required. All PCRs were performed with the enzyme BD Advantage2 (Clontech). "Touchdown" PCR parameters were used for the first-round RACE reaction; all other PCRs were performed under standard conditions (Clontech). The amplified fragments were gel-extracted (Qiagen) and ligated into a suitable vector before sequencing (MWG Biotech). The cDNA was aligned to *mgl* sequences using BLASTn (NCBI) and Wormbase.

Rescue Experiments

The cosmid ZC506 was used to perform *mgl-1(tm1811)* rescue experiments and was supplied by the *Caenorhabditis* Genetics Centre. The cosmid ZC506 (at 10–15 ng/μl) was coinjected with the *myo-2::GFP* reporter plasmid pPD11833 (obtained from A. Fire) at 20–30 ng/μl. The expression of GFP in the pharyngeal muscle was used to screen for transgenic lines expressing ZC506.

Generation of the Peat-4::ChR2;mRFP Integrated Strain

ChR2 was amplified from the plasmid *Pmyo-3::ChR2-(H134R);YFP* using the primers 5′-CTAGAGACTAGTATGGATTATGGAGGGCCTG (forward) and 5′-ATGGGGTACCTTAG GGCACCGCGCCAGCCTCGGCCTC (reverse). The reverse primer contained a synonymous substitution that removed a KpnI site internal to ChR2 and introduced an artificial stop codon. ChR2 was cloned SpeI/KpnI upstream of mRFP in the gateway entry vector p-ENTR. This was recombined with the gateway destination vector, p-DEST, containing 6 kb of *eat-4* promoter to generate the construct *Peat-4::ChR2;mRFP*. The construct *Peat-4::ChR2;mRFP* was injected at a concentration of 50 ng/μl. Lines were established from the F2 generation stably expressing *mRFP*. *Peat-4::ChR2;mRFP* was integrated by UV irradiation and outcrossed six times.

Construction of the mgl-2::GFP and mgl-3::GFP Gene Reporter

For the *mgl-2::GFP* reporter construct, the primers 5′-CATGCATGCAAGCAAACTGAAAATCGCTCCGTGG and 5′-CAAGGTACCTTCGCCGCGTTTTTGCTCTTTTCTAC were used to amplify ~4.5 kb of *mgl-2* promoter. This was cloned into the fire vector pPD95-75 using the restriction sites Sph1/Kpn1. Using the primers 5′-GTTGGTACCAATGGTGTAGCTTGAGACAGC-3′ and 5′-CAAGGTACCATGCTCTACAGTCATGTCACAC-3′, the full-length cDNA encoding MGL-2 (F45H11.4 in WS243) was amplified, TOPO-cloned (Invitrogen), and cut using the enzyme KpnI. The 5′ KpnI site was incorporated into the 5′ primer, whereas the 3′ site was internal to the MGL-2 coding sequence and located within the C terminus. This product was cloned downstream of the *mgl-2* promoter in the vector pPD95-75 using the KpnI restriction site to generate an MGL-2 protein fusion to GFP at the C terminus. This was injected at 20 ng/μl into the N2 strain by standard techniques (30).

For the *mgl-3::GFP* reporter construct, the primers *5′-TTCGTCGACAATAGTATTCCCGAGAACGG* and *5′-GCGGCCGCTTTTACTGTCGAACTGATTGG* were used to amplify ~5 kb of *mgl-3* promoter and the first exon (containing the first putative start codon). This fragment was cloned upstream of *GFP* in the vector pHAB*GFP* (provided by Howard Bayliss) using the restriction sites SalI and NotI to generate the construct *mgl-3::GFP*. This was coinjected at 10–20 ng/μl with the *pha-1* rescue plasmid pBX (obtained from R. Schnabel) into the temperature-sensitive strain *pha-1(e2123)* by standard techniques (30). Transformed lines were selected under temperature-sensitive conditions (25.5 °C).

Imaging of the mgl::GFP Reporter Strains

Animals were mounted in a 5 μl drop of 10 mM levamisole (Sigma) on a 2% agarose pad covered with a 24 × 24 mm coverslip. Differential interference contrast and fluorescence imaging were performed on a Nikon Eclipse TE800 fluorescence microscope equipped with a Hamamatsu C4742-95 digital camera. Confocal images were captured with a Zeiss LSM-510 laser-scanning microscope.

Electropharyngeogram (EPG) Recordings

Hermaphrodite animals were grown on a bacterial lawn of OP50, and young adults were picked for electrophysiological experiments. Animals were placed into a Petri dish containing modified Dent's saline (10 mM glucose, 5 mM HEPES, 140 mM NaCl, 6 mM KCl, 3 mM $CaCl_2$, and 1 mM $MgCl_2$ (pH7.4)) supplemented with bovine serum albumin (0.1% w/v). Worms were dissected by cutting them at the pharyngeal-intestinal valve with a razor blade, causing the cuticle to retract and exposing the isthmus and terminal bulb to generate a semi-intact pharyngeal preparation in which the pharyngeal microcircuit remained intact. The dissected preparation will have a distinct physiology compared with the intact organism, where the somatic nervous system was completely intact. All experiments were performed at room temperature (≈ 20–22 °C). The pharyngeal preparation was transferred to a custom-made recording chamber (volume, 1 ml) mounted on a glass coverslip. Suction pipettes were pulled from borosilicate glass (glass

diameter, 1 mm; tip diameter, ≈12 μm; Harvard Instruments). The pipette was lowered into the recording chamber and placed close to the anterior end of the preparation. Suction was then applied to attach the preparation to the pipette. The suction pipette was attached to an Axoclamp 2B recording amplifier. The reference electrode was a silver chloride pellet in Dent's saline connected to the recording chamber by an agar bridge. Extracellular voltage recordings were made in "bridge" mode, and the extracellular potential was set to 0 mV using the voltage offset immediately prior to recording. Data were acquired using Axoscope (Axon Instruments) and stored for subsequent offline analysis.

In single-dose experiments, the recordings were made from the pharynges in Dent's saline for 5 min. The drug was then applied to the semi-intact pharyngeal preparation by removing and replacing the solution using a 1-ml pipette. Recordings were made from the pharynx in the presence of drug for 5 min, and then the drug was washed off. The frequency of the EPGs was measured for 5 min before drug application and 5 min after drug application. The drug was then washed off the preparation. After the drug was washed off, the preparations of EPGs were measured for a further 5 min in Dent's saline. Following the 5 min recovery period in Dent's saline, 500 nM 5-HT was applied by removing and replacing the Dent's saline using a 1-ml pipette. EPGs were measured for a further 2.5 min in the presence of 5-HT. The duration of the entire experiment for a single worm did not exceed 25 min, including the time taken to dissect the worm pharynx and apply the suction electrode.

The LCCG-I concentration-response curve was generated by sequentially applying increasing concentrations of drug to the dissected semi-intact pharynges. The addition of each concentration was preceded by a 5-min recovery period in Dent's saline. The drug was applied for 2.5 min, and the EPGs were measured during this period. The effect of the drug on the frequency of pharyngeal EPGs was expressed as a percentage change compared with the basal resting rate during the 2.5 min immediately before the addition of the drug. The duration of the entire experiment for a single worm did not exceed 77.5 min for mgl-1and 62.5 min for N2, including the time taken to dissect the worm pharynx and apply the suction electrode.

Intracellular Recordings

The dissected pharynx was transferred to a custom-built perfusion chamber (volume, 1 ml) on a glass coverslip. The recording chamber was mounted on a microscope stage and perfused via gravity feed with saline at a rate of 20 ml min^{-1}. The preparation was secured with a glass suction pipette applied to the terminal bulb region of the pharynx and then impaled with an aluminosilicate glass microelectrode (1.0-mm outer diameter) pulled on a microelectrode puller to tip with a resistance of 60–80 MΩ, filled with 4 M potassium acetate and 10 mM KCl, and connected to an Axoclamp 2A amplifier. The reference electrode was a silver chloride-coated silver pellet in 3 M KCl connected to the recording chamber by an agar bridge. Data were acquired and analyzed using PClamp8 (Axon Instruments). Drug solutions were diluted with Dent's saline from stocks as required.

Electrophysiological Recording of the Peat-4::ChR2;mRFP Light-evoked Response

The strains N2;*Is[Peat-4::ChR2;mRFP]*, *mgl-1(tm1811);Is-[Peat-4::ChR2;mRFP]*, and *eat-4(ky5);Is[Peat-4::ChR2;mRFP]* were subjected to pharyngeal dissection as in Ref. 31. Desheathed pharynges were placed in a recording chamber and illuminated using a blue light-emitting diode with a wavelength of 470 nM as described in Ref. 31). Intracellular recordings of muscle action potentials were recorded from the terminal bulb using sharp electrodes (as described above). For N2; *Is[Peat-4::ChR2;mRFP]* and *mgl-1(tm1811);Is[Peat-4::ChR2; mRFP]*, recordings were made in the presence and absence of LCCG-I. The last ten light stimuli for each phase of the experimental time course were analyzed.

Chemicals

(±)-1-Aminocyclopentane-trans-1,3-dicarboxylic acid ((±)trans-ACPD) (catalog no. 0187), and (2S,1′S,2′S)-2-(carboxycyclopropyl)glycine (LCCG-I, catalog no. 0333) were obtained from Tocris Biosciences (Bristol, UK). All other chemicals were obtained from Sigma or Fisher.

Pharyngeal Pumping Assays in Intact Animals

A synchronized population of young adult worms was generated by picking L4-staged animals to a fresh food plate 16–18 h before performing the assay. For each individual animal, the number of pumps performed within 1 min on food was counted, and the food was then removed by placing the animal onto a fresh non-food plate and allowing it to move around for 1 min. Individual animals were transferred to a separate, second non-food plate, and the number of pumps (defined as the number of backward movements of the terminal bulb grinder) performed in 1 min were counted at two time points, 5 min and 95 min following the transfer. Then, after 96 min, worms were returned to food, and, at 100 min, the pharyngeal pumping was recorded.

Data Analysis

The results are expressed as the percentage change in frequency ± S.E. of the mean for *n* individual pharynxes. For the EPG recordings, each drug was tested on a separate pharynx. Significance was measured using one-way analysis of variance with Bonferroni post test, unless stated otherwise. Concentration-response curves were plotted by fitting the data to the modified logistic equation (GraphPad Prism, San Diego, CA), and EC_{50} values are given with 95% confidence limits.

Results

Molecular Organization of MGL Subtypes—A combination of PCR-mediated approaches (RACE, SL-1/2 amplifications, and predictive PCR; see "Experimental Procedures" for further details) were applied to either of two cDNA pools prepared independently from mixed-stage animals (see "Experimental Procedures") to characterize the 5′ and 3′ ends of the *mgl* cDNAs. The combined findings of these different approaches have been published elsewhere (32) and are presented in summary here, together with a revised annotation for *mgl-2* on the

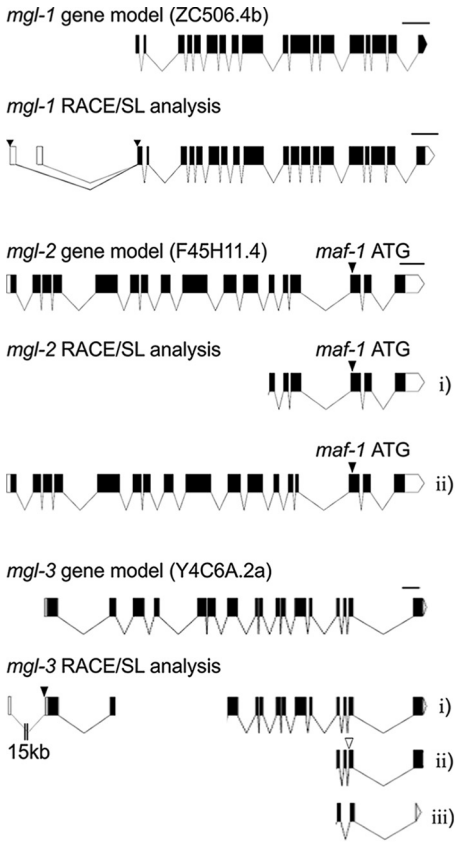

FIGURE 1. **Molecular characterization of the different *mgl* receptor subtypes.** Exon-intron boundaries characterized by the analysis of SL-1 PCR-amplified and RACE-amplified cDNA fragments are shown for each *mgl* subtype. For comparison, the gene models annotated by Wormbase version WS243 are shown. ▼, SL-1 *trans*-splice site; ▽, alternative splice donor site leading to a six-nucleotide insertion. The position of the putative *maf-1* ATG start codon is indicated in the diagram of the *mgl-2* gene models. *White boxes* represent 5′ and 3′ untranslated regions. *Scale bars* = 500 bp.

basis of further analysis. The *mgl-1* gene encodes at least three different 5′ isoforms, two of which are alternatively *trans*-spliced to SL-1, the nematode specific *trans*-splice leader. One of the SL-1 *trans*-spliced variants supports the 5′ gene structure currently defined for *ZC506.4b*. The other SL-1 *trans*-spliced variant (European Nucleotide Archive accession no. LN681209) and 5′RACE analysis (European Nucleotide Archive accession no. LN681208) identified an alternative 5′ gene structure (Fig. 1). The sequence of the putative signal peptide predicted from the translated 5′ cDNA sequences of each of the *mgl-1* isoforms suggests that each of the 5′ variants use the same ATG as its start codon. The 3′RACE amplification identified a single *mgl-1* C-terminal variant and redefines exon 11 of *ZC506.4b* (European Nucleotide Archive accession no. LN681210) (Fig. 1).

A single *mgl-2* 5′ isoform was identified that was not *trans*-spliced to the SL-1 sequence (attempts to amplify *mgl-2* 5′ cDNA using SL-1 and SL-2 complementary primers were unsuccessful). The 3′ cDNA analysis suggests that *mgl-2* encodes at least two different 3′ isoforms. Predictive PCR identified that alternative splicing creates a long and a short C-terminal variant (denoted *mgl-2i* and *mgl-2ii*, respectively). The long C-terminal variant (*mgl-2i*) corresponds to the transcript currently defined in Wormbase (transcript F45H11.4, Wormbase version WS243). The 3′ RACE analysis covered an extended region of the *mgl-2* gene compared with the predictive PCR and confirmed the alternative splicing in *mgl-2ii* (Fig. 1). In our analysis, we discovered that the ORF of *mgl-2ii* and the downstream gene, *maf-1*, were contained within a single transcript. This was confirmed by the amplification of a single transcript using primers designed against the *maf-1* 3′ end and *mgl-2* 5′UTR. Sequencing of this transcript confirmed both the alternative splicing in *mgl-2ii* and a four-nucleotide overlap (ATGA) between the 3′ end of *mgl-2ii* and the 5′ end of *maf-1* that contains the putative TGA stop codon for *mgl-2ii* and the putative ATG start codon for *maf-1* (European Nucleotide Archive accession no. LN681207). The ORFs of *mgl-2ii* and *maf-1* were not in-frame with each other, and *in silico* translation in their respective reading frames gave rise to a *bona fide* protein sequence.

At least two different *mgl-3* 5′ isoforms were identified, the difference being that one variant was SL-1 *trans*-spliced (European Nucleotide Archive accession no. LN681212), whereas the other contained a predicted untranslated exon within the 5′ promoter region, located ≈15 kb upstream of the first coding exon (European Nucleotide Archive accession no. LN681211) (Fig. 1). The analysis of the C terminus of *mgl-3* suggests that it undergoes alternative splicing, giving rise to at least three different C-terminal splice variants (*mgl-3i/ii/iii*) (Fig. 1). In *mgl-3ii* (European Nucleotide Archive accession no. LN681214). Exon 16 uses an alternative splice donor site compared with *mgl-3i/iii* that incorporates six additional nucleotides that are otherwise intronic in *mgl-3i* (European Nucleotide Archive accession no. LN681213) and *mgl-3iii* (European Nucleotide Archive accession no. LN681215). The result of this is the substitution of a threonine residue for the amino acid triplicate ISA. Other than this, the sequence of the *mgl-3i/ii* 3′ cDNA region that was PCR-amplified was the same. In *mgl-3iii*, alternative splicing caused a frameshift in the downstream open reading frame and the introduction of an alternative stop codon. The isoform *mgl-3iii* has been identified independently by EST submission EC001043. The 3′ RACE analysis of the *mgl-3* C-terminal confirmed the *mgl-3i* splice variant (European Nucleotide Archive accession no. LN681216).

The molecular phylogeny of the MGR family provided in this study is an updated analysis and a further clarification of that published previously (32). It supports the assignment of the three nematode MGL proteins to the three mammalian MGR types (Fig. 2). MGL-2 forms a well supported clade with vertebrate group I (>99% bootstrap support). MGL-1 has classified previously weakly as group I-like (32, 33), but phylogenetic analysis (and BLASTP results) show that it is actually more closely related to vertebrate group II sequences (>97% bootstrap support). MGL-3 is most similar to group III sequences (Fig. 2, >80% bootstrap support). Although none of the insect species with fully sequenced genomes to date have all of the MGR types, sequences from different insects indicate that there may be four subfamilies. mGluRB (FBpp0271833) (also known as DmXR or mangetout), is not a glutamate receptor, however, and it has been suggested that it has diverged from the rest of the family to recognize a different ligand that is not a natural amino acid (34). It is not known whether the sea urchin ortho-

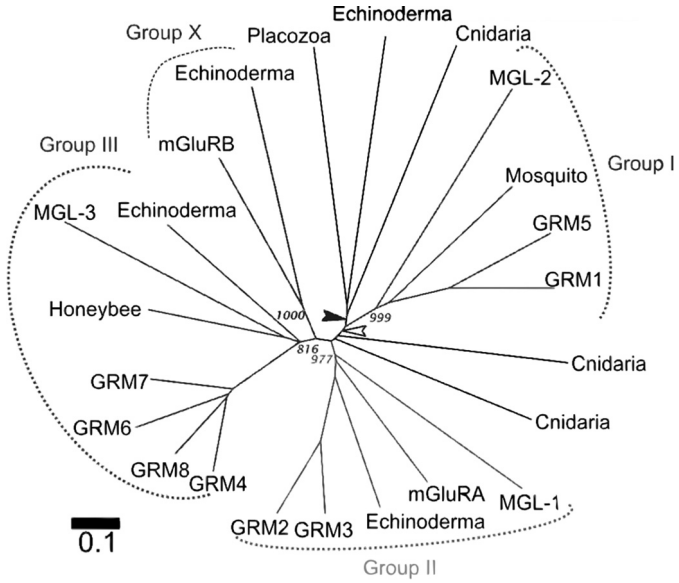

FIGURE 2. **Unrooted molecular phylogeny of the mGluR family with subfamily clades represented by single branches for clarity.** The root position using vertebrate taste receptors as an outgroup (not shown) is indicated by a *filled arrow*. The position given by midpoint rooting of the mGluR family alone is indicated with an *open arrow*. Bootstrap values for the main MGR groups are shown (1000 replicates). Vertebrate mGluR GRM1–8, nematode MGL1–3, and *Drosophila* mGluRA and mGluRB are labeled. Other sequences are indicated with taxa only.

logue (SPU_017426tr) is recognized by glutamate, but the topology and presence of four echinoderm GluR sequences is consistent with this "group X" subfamily being lost in the chordate lineage rather than gained in the insect lineage. Although not conclusive, this analysis suggests that group X is most closely related to group III (77% bootstrap support). Consistent with previous studies in *C. elegans*, none of the fully sequenced nematodes analyzed had a group X receptor.

Distinct and Overlapping Expression Patterns for the Three mgls in C. elegans—To assess and compare the expression patterns of each of the three *mgls* in *C. elegans*, transgenic animals expressing extrachromosomal fusions to GFP were constructed for *mgl-2* and *mgl-3* (see "Experimental Procedures"). For *mgl-1*, a gene fusion to GFP was generated independently (see "Experimental Procedures"), and analysis was performed on animals stably expressing the *mgl-1::GFP* as an integrated array. Of the three receptors, *mgl-1* appeared to have the most widespread expression pattern. The reporter *mgl-1::GFP* was expressed extensively in the nerve ring, in tail neurons, and extensively within the pharyngeal nervous system, which included the neurosecretory motor neuron NSML/R, interneurons, and motor neurons (Fig. 3, *A–C*). In worms expressing *mgl-2::GFP* as an extrachromosomal array, GFP fluorescence was identified in the nerve ring, tail neurons, and the pharyngeal nervous system, where it was expressed in NSML/R (Fig. 3, *D–F*). The analysis of *mgl-2::GFP* transgenic lines also identified GFP expression in the glutamatergic pharyngeal neuron I5, the anterior and posterior intestine, the pharyngeal-intestinal valve, and pharyngeal muscle. However, the expression of GFP in these tissues was not consistent between the transgenic lines analyzed. In worms expressing *mgl-3::GFP* as an extrachromosomal array, GFP fluorescence was detected in the pharyngeal

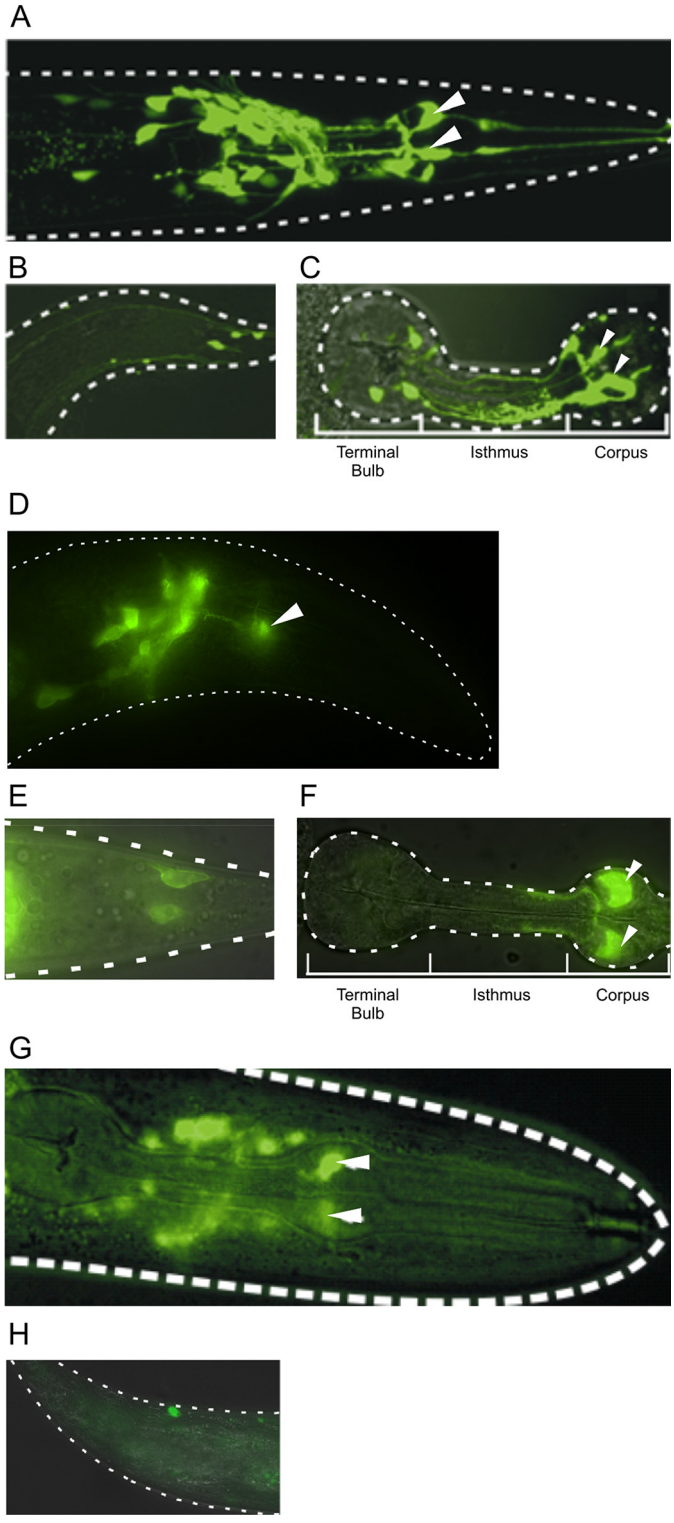

FIGURE 3. **The *mgl* subtypes have distinct and overlapping expression patterns in the *C. elegans* nervous system**. *A–C*, the expression of *mgl-1::GFP*. *A*, nerve ring; *B*, tail; *C*, pharyngeal nervous system. *D–F*, the expression of *mgl-2*::GFP. *D*, nerve ring; *E*, tail; *F*, the pharyngeal nervous system. *G–H*, the expression of *mgl-3*::GFP. *G*, nerve ring and pharyngeal nervous system; *H*, tail. The *white dotted lines* indicate the outer perimeter of the preparation of the whole worm (*A*, *B*, *D*, *E*, *G*, and *H*) and the unsheathed pharyngeal preparation (*C* and *F*). The pharynx was desheathed by removing the overlaying cuticle and muscle. Each of the *mgl* subtypes is expressed in the pharyngeal NSM neurons, indicated by *white arrowheads*.

nervous system, specifically NSML/R, and in the nerve ring (Fig. 3*G*).

Pharmacological Characterization of mgls Using EPG Recording in the Pharynx—To further investigate whether *mgl* receptors control pharyngeal pumping, an electrophysiological assay was developed using mGluR agonists that have a well characterized efficacy at mammalian mGluRs (35) and have been shown previously to exert activity on invertebrate nervous systems (14, 15).

The EPG is an extracellular recording technique that enables the detection of electrical transients in the pharyngeal muscle and associated circuit of 20 neurons, which are embedded underneath the basement membrane. The myogenic activity of the pharyngeal muscle is modulated by the activity of the pharyngeal nervous system (36). In the experiments described here, an incision is made at the pharyngeal-intestinal valve, leading to the extrapharyngeal nervous system being displaced (Fig. 4*A*) and leaving the embedded pharyngeal neurons that express *mgl-1*, *mgl-2*, and *mgl-3*. This ensures that the drug response is driven either by the action of receptors expressed in pharyngeal neurons or by direct activation of the underlying pharyngeal muscle.

EPG recordings were made from wild-type animals to look at the effect of mammalian mGluR agonists on the electrophysiology and pumping behavior of the pharynx (Fig. 4). (±)*trans*-ACPD is a mammalian mGluR agonist with broad-spectrum activity against the distinct subclasses of receptors (35). Pharmacological profiling of representative mGluR group members suggests that (±)*trans*-ACPD is a potent agonist of group I (EC_{50} = 15 μM at mGluR1) and group II receptors (EC_{50} = 2 μM at mGluR2) and a weak agonist at group III receptors (EC_{50} = 800 μM at mGluR4) (35).

Initially, 100 μM (±)*trans*-ACPD was applied to the wild-type preparation. (±)*trans*-ACPD is an equimolecular mixture of (1S,3R)- and (1R,3S)-ACPD and a selective agonist for mGluRs. A variable response was obtained that consisted of a large increase, no change, or an inhibition of the basal pumping frequency (data not shown). At the increased concentration of 500 μM, which is more in keeping with the EC_{50} of this agonist at group III mGluRs, (±)*trans*-ACPD consistently caused a reversible inhibition of basal pumping in wild-type pharynges (Fig. 4*B*). In a high proportion of animals, a rebound excitation was recorded during the first few minutes of the recovery period, after the drug was washed off (Fig. 4*B*). The neurotransmitter 5-HT is known to be a potent stimulator of pharyngeal pumping (37, 38). Following the wash period, 500 nM 5-HT was applied to assess the viability of the pharynx at the end of the recordings. In each recording, the application of 500 nM 5-HT caused a potent stimulation of pharyngeal pumping, confirming that the pharyngeal circuit was still capable of high-frequency pumping after (±)*trans*-ACPD had been applied and following a 5-min wash period (Fig. 4*B*). LCCG-I is a more potent broad-spectrum mGluR agonist than (±)*trans*-ACPD and has a higher potency at the mGluR II and III subgroups. The EC_{50} at representative group I, II, and III mGluRs is 50 μM (mGluR1a), 1 μM (mGluR3), and 9–50 μM (mGluR4a), respectively (35). The application of 100 μM LCCG-I to the wild-type pharynx preparation caused a consistent and reversible inhibi-

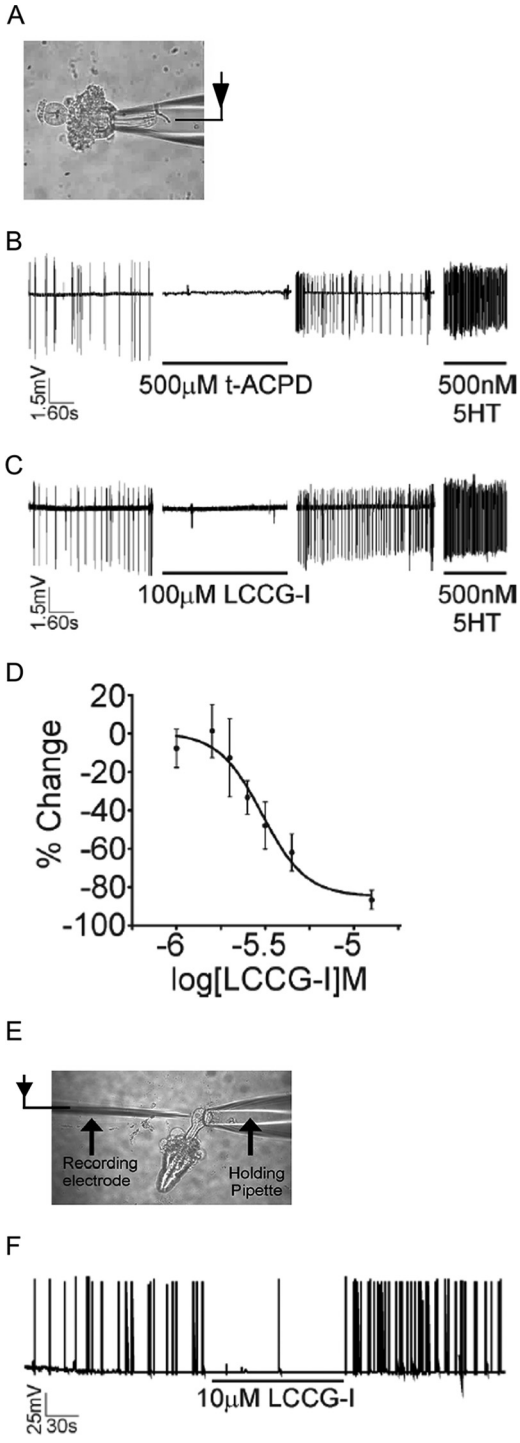

FIGURE 4. **The selective mGluR agonists *trans*-ACPD and LCCG-I both inhibit the activity of the pharyngeal neuromuscular network.** *A*, EPG recording configuration from the semi-intact pharyngeal preparation. *B* and *C* each show an EPG recorded from individual pharynges of wild-type worms. Each deflection represents a single pharyngeal pump (because of the long time base, individual pumps cannot always be resolved if the pumping activity is fast). The period of drug application is indicated on individual recordings. *D*, concentration-response curve for the effect of LCCG-I on the percentage change in the rate of pharyngeal pumping recorded in the EPG configuration. Each point is the mean ± S.E. of nine determinations. *E*, intracellular recording configuration to measure pharyngeal muscle activity. *F*, the effect of 10 μM LCCG-I on the frequency of pharyngeal action potentials recorded intracellularly from the *C. elegans* pharyngeal terminal bulb muscle. The period of drug application is indicated on the recording by the *solid black line*, with the concentration indicated beneath.

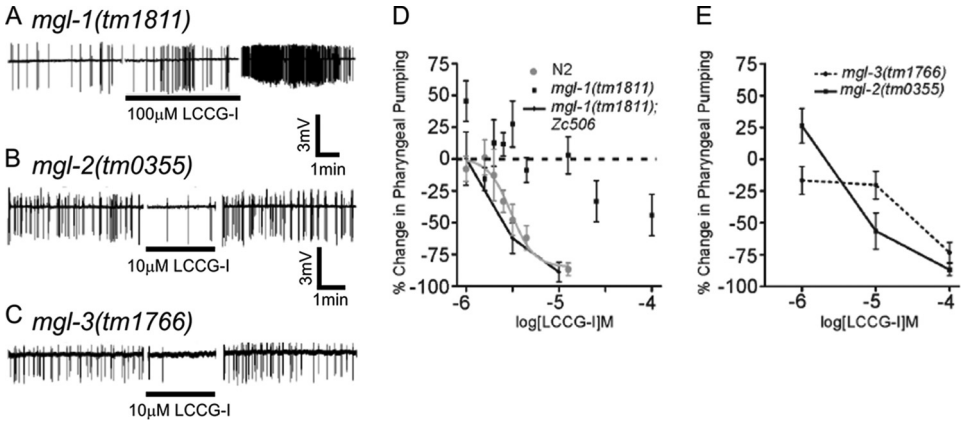

FIGURE 5. **The effects of LCCG-I on the EPG recorded from the pharyngeal muscle of *mgl* receptor subtype mutants.** *A–C*, EPGs recorded from individual *mgl* mutant pharynges. The point of LCCG-I drug application is indicated on individual recordings by solid lines, with the concentration indicated beneath. *D*, concentration response of *mgl-1(tm1811)* and the genomic rescue *mgl-1(tm1811);ZC506* (the wild-type response is included for comparison). For *mgl-1(tm1811)*, each point is the mean ± S.E. of 12 determinations. For the *mgl-1(tm1811)* genomic rescue, 10 individual pharynxes were tested (five from each of two stable transgenic lines transformed with ZC506). Each point is the mean ± S.E. of 10 determinations. *E*, concentration response for the effects of LCCG-I on *mgl-2(tm0355)* and *mgl-3(tm1766)*. Each point is the mean ± S.E. of six determinations for *mgl-2(tm0355)* and five for *mgl-3(tm1766)*.

tion of the EPGs that was often complete for the period of drug exposure (Fig. 4*C*). For the same reasons as described previously, 500 nM 5-HT was applied to the pharynx after LCCG-I had been applied and after a 5 min wash period. In each recording, the application of 500 nM 5-HT caused a potent stimulation of pharyngeal pumping, confirming that the pharyngeal circuit was still viable and retained the sensitivity to 5-HT. The EC_{50} for the inhibition of pharyngeal pumping by LCCG-I was measured at 3 μM in the dose-response analysis (Fig. 4*D*).

The intracellular recording configuration enables the measurement of pharyngeal muscle activity (Fig. 4*E*). Compared with the EPG, it provides a more direct measure of pharyngeal pumping and its modulation by the embedded pharyngeal nervous system. In such recordings, 10 μM LCCG-I caused an inhibition of spontaneous action potential firing. However, the resting membrane potential (−75mV) was not changed by addition of the drug (Fig. 4*F*). The latter supports the expression studies that failed to detect receptors in the muscle, arguing against a direct effect of LCCG-I on this tissue. Rather, the intracellular recordings indicate that LCCG-I activates receptors that reside within the pharyngeal nervous system and modify network activity that supports pharyngeal pumping. The potency of LCCG-I (EC_{50} = 3 μM) suggest a specificity at the group II-like MGL receptor (MGL-1), but we extended the analysis to investigate pharmacological activation by LCCG-I in the various *mgl* mutants.

LCCG-I Modulation of Network Activity across mgl Mutants—Deletion alleles exist for each of the three *mgl* receptors. These are *mgl-1(tm1811)*, *mgl-2(tm0355)*, and *mgl-3(tm1766)*. The mutations were confirmed by PCR using both genomic DNA and cDNA derived from the *mgl* mutants. DNA sequencing of the amplified PCR products confirmed that, in each case, the deletion culminates in a putative null (data not shown).

To probe the basis of the mGluR agonist activity in the wild-type pharyngeal preparation, EPGs were conducted on the *mgl* mutants in the presence of each agonist. (±)*trans*-ACPD was only tested on *mgl-1(tm1811)* at 500 μM, and pumping by these animals was not impaired by the drug as in the wild type (data not shown). LCCG-I was tested over a range of concentrations on each of the *mgl* mutants (Fig. 5, *A–C*). EPGs by *mgl-1(tm1811)* animals were not inhibited over the range of 1–12.5 μM, but, at the higher concentrations tested (25 and 100 μM), a partial inhibition began to be observed (Fig. 5*D*). In contrast to *mgl-1(tm1811)*, both *mgl-2(tm0355)* and *mgl-3(tm1766)* EPGs were strongly inhibited by concentrations of LCCG-I at 3 μM and 10 μM (Fig. 5*E*), suggesting that *mgl-1* is primarily responsible for the LCCG-I response. The wild-type response of pharynges to LCCG-I was restored in *mgl-1(tm1811)* by injecting cosmid DNA (10–15 ng/μl) (Fig. 5*D*) containing the entire *mgl-1* genomic sequence and ≈3.6 kb of sequence upstream of the first non-coding exon defined by the RACE analysis (Fig. 1). This provides further support for the hypothesis that *mgl-1* is responsible for the inhibitory effect of LCCG-I on the pharynx.

At the lower range of LCCG-I concentrations tested (1 μM), an increase in the frequency of EPGs was measured from both *mgl-1(tm1811)* and *mgl-2(tm0355)* (Fig. 5, *D* and *E*, respectively) but not *mgl-3(tm1766*). Instead, *mgl-3(tm1766)* was inhibited by LCCG-I without the low-dose activation seen at 1 μM (Fig. 5*E*). Therefore, *mgl-3* appears to increase the frequency of pharyngeal pumping at low concentration. The modulation of the pharyngeal network in an *mgl-1*- and *mgl-3*-dependent manner further supports the expression of these receptor subtypes within this microcircuit.

Optogenetic Activation of Glutamatergic Evoked Activity in the Pharyngeal Network Is Modulated by LCCG-I—Next we wanted to identify whether the presynaptic activation of *mgl-1* within the pharyngeal nervous system inhibited glutamate-initiated changes in the activity of the postsynaptic pharyngeal muscle. Optogenetics enables the discrete activation of specific subsets of neurons within a network. Therefore, an optogenetic approach was used to selectively depolarize neurons capable of glutamate release within this network. Light-evoked changes in the activity of the pharyngeal network were measured by making simultaneous intracellular recordings from the pharyngeal muscle, which is the postsynaptic target of the pharyngeal neural network. This optogenetic electrophysiological approach

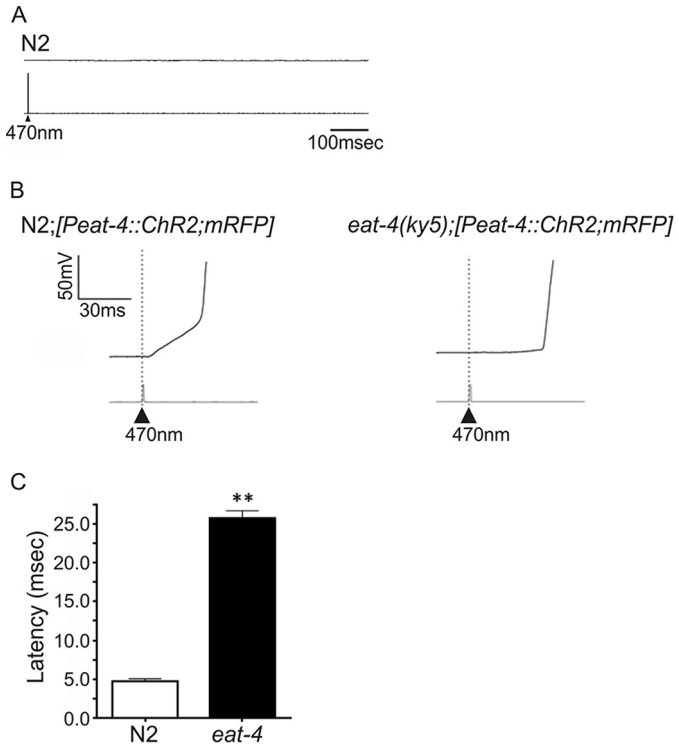

FIGURE 6. **A comparison of excitatory pharyngeal muscle responses in the desheathed pharyngeal preparation of wild-type (N2) and glutamate-deficient (*eat-4*) worms following optogenetic activation of glutamatergic pharyngeal neurons.** *A*, representative trace to show that a 1-ms pulse of blue light (470 nm) did not excite the pharynx of N2 worms that do not express *Peat-4::ChR2;mRFP*. The stimulus is indicated in the trace below the voltage response recorded from the muscle. *B*, representative traces of the light-stimulated postsynaptic potentials recorded from the pharyngeal muscle of N2 and *eat-4(ky5)* worms expressing *Peat-4::ChR2;mRFP*. Note that the postsynaptic response still occurs in *eat- 4(ky5)*, but the latency is longer. *C*, the latency of the light-activated PSP is significantly longer in *eat-4(ky-5)* compared with N2. *eat-4(ky5);[Peat-4::ChR2;mRFP]* ($n = 8$) and *N2;[Peat-4::ChR2;mRFP]* ($n = 14$). Results are presented as the mean ± S.E. **, $p < 0.01$ in an unpaired Student's *t* test.

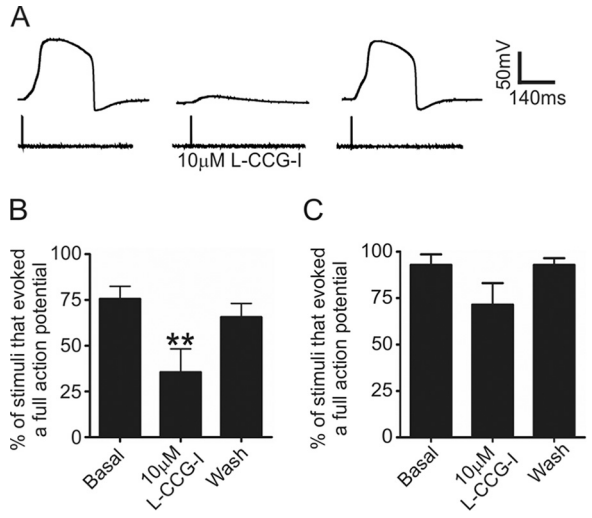

FIGURE 7. **The effect of LCCG-I on light-evoked postsynaptic potentials in the desheathed pharyngeal preparation of wild-type and *mgl-1(tm1811)* worms.** *A*, representative light-evoked postsynaptic responses in N2 wild-type worms expressing *Peat-4::ChR2;mRFP* before, during, and after the application of 10 μM LCCG-I. The stimulus is indicated in the trace below the voltage response recorded from the muscle. *B* and *C*, quantification of the LCCG-I inhibition of full action potentials evoked by light activation of *Peat-4::ChR2* in wild-type (*B*, $n = 10$) and *mgl-1(tm1811)* (*C*, $n = 7$) worms. A postsynaptic potential was considered to be light-evoked when it occurred within 50 ms of the stimuli, otherwise it was considered as arising from the spontaneous intrinsic activity of the pharynx and was not included in the analysis.

was combined with the pharmacological activation of *mgl-1* using the agonist LCCG-I.

The optogenetic depolarization of glutamatergic neurons was achieved by using an integrated line in which the light-sensitive channel rhodopsin (ChR2) was expressed under the control of the *eat-4* vesicular glutamate transporter promoter (*Peat-4::ChR2;mRFP*). The expression of this construct is widespread in the *C. elegans* nervous system but restricted to M3, NSM, I2, and I5 in the pharynx (48), consistent with its expression in the glutamatergic neurons. Worms were cultured on NGM plates containing retinal, an essential cofactor required for ChR2 activation. A 1-ms pulse of light (470 nm) did not excite the exposed pharynx of N2 worms that had not been transformed with *Peat-4::ChR2;mRFP* (Fig. 6*A*) (31). Light activation of the exposed pharynx of wild-type worms expressing *Peat-4::ChR2;mRFP* produced a tightly coupled light-evoked excitation in the pharyngeal muscle (Fig. 6*B*). The light-activated response is initiated from the glutamatergic neurons of the circuit. However, the evoked response measured at the muscle involves a complex depolarization usually followed by a superimposed action potential. The complexity of the response arises because the pharyngeal glutamatergic neurons produce activity in the circuit via gap junctions and the release of transmitters in addition to glutamate. These interactions are the major determinant of the complex response that is recorded in the muscle (31, 48). This expected observation is reinforced by the fact that, although the light induced response is delayed, it is not prevented when it is triggered in the pharynx of *eat-4* mutant animals that lack glutamate release but retain other activities independent of glutamate release (Fig. 6, *B* and *C*).

To determine whether *mgl-1* inhibits the light-activated response, the optogenetic electrophysiological experiments were combined with the pharmacological activation of *mgl-1*. 10 μM LCCG-I was bath-applied, and light-evoked recordings were made from the exposed pharynges of wild-type worms expressing *Peat-4::ChR2;mRFP*. As in the previous pharmacological experiments that used intrinsic activity, the application of LCCG-I at a dose (10 μM) that is selective for the *mgl-1*-mediated inhibition caused a reduction in the percentage of the light-evoked pharyngeal muscle depolarization (Fig. 7, *A* and *B*). This LCCG-I inhibition of the light-evoked pharyngeal depolarization was reversed upon washout. LCCG-I often reduced the rise of the light-induced response but, the complex nature of this initial depolarization limits the use of this parameter as a measure of the drug effect. In contrast, the inhibition by LCCG-I was clearly quantified by comparing the almost complete inhibition of the light-evoked pharyngeal action potentials that were otherwise seen frequently when light activation was performed in the absence of the drug (Fig. 7, *A* and *B*). The inhibition of the light-evoked pharyngeal muscle response by LCCG-I was reversed to almost wild-type levels during the wash phase (the basal and wash periods were not significantly different in a paired Student's *t* test).

Light-evoked recordings were then made from the exposed pharynx of *mgl-1* worms expressing *Peat-4::ChR2;mRFP* in the

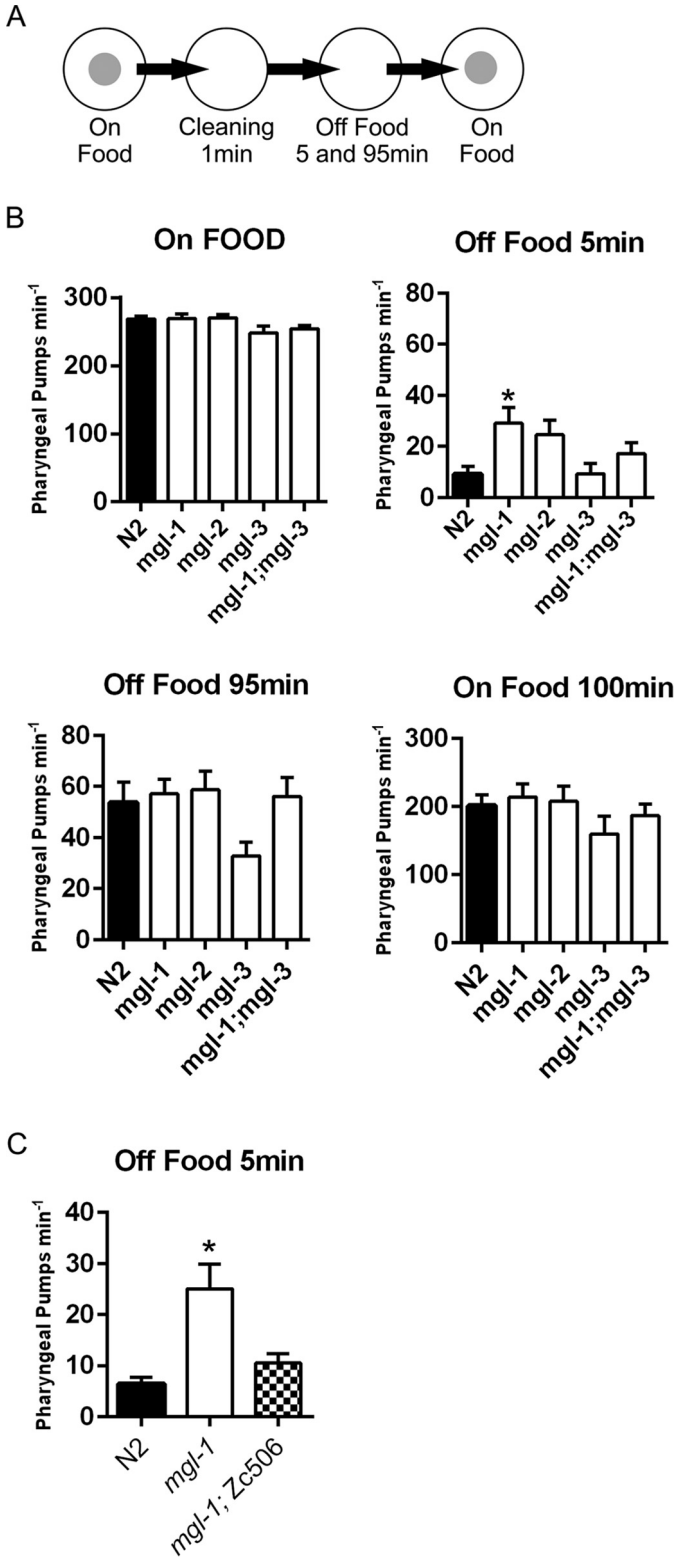

FIGURE 8. **The effect of acute and longer-term food deprivation upon the regulation of pharyngeal pumping in *mgl* mutant animals.** *A*, diagram indicating the time line of the pharyngeal pumping assay. *B*, the rate of pumping on and off food at the time points indicated in *A* for N2 ($n = 39$), *mgl-1(tm1811)* ($n = 27$), *mgl-2(tm0355)* ($n = 28$), *mgl-3(tm1766)* ($n = 17$), and *mgl-1(tm1811);mgl-3(tm1766)* ($n = 30$). Significance was determined using one-way analysis of variance and Bonferroni post test comparisons to compare *mgl* mutant pumping with wild-type pumping. *, $p < 0.05$ in Bonferroni post test comparisons. *C*, the rate of pumping 5 min after removal from food to assess rescue against the *mgl-1* exaggerated OFF-food phenotype by the cosmid ZC506. N2 ($n = 15$), *mgl-1(tm1811)* ($n = 15$) and the rescue *mgl-1(tm1811);ZC506* ($n = 15$). Significance was determined using unpaired Student's *t* test to compare *mgl-1(tm1811)* and *mgl-1(tm1811);ZC506* to wild-type pumping.

absence and presence of LCCG-I. The percentage of stimuli that evoked a full action potential in the absence of LCCG-I during the basal period and then in the presence of 10 μM LCCG-I was not significantly different in the *mgl-1(tm1811)* mutant background (Fig. 7*C*). This suggests that *mgl-1* activation is largely responsible for the LCCG-I-mediated inhibition of light-evoked changes in the network activity.

Modification of Modulatory Tone Associated with an Adaptive Response to Food Deprivation in Intact Animals Lacking mgl Subtypes—The pharmacological detection of *mgl-1* as an inhibitor of pharyngeal pumping suggests that it may be involved in the modulation of *C. elegans* feeding behavior. Experiments in the isolated pharynx and whole organism represent a significant transition from an *in vitro* to an *in vivo* analysis. The modulation of the activity in the isolated pharynx is largely restricted to the embedded pharyngeal nervous system, whereas the intact worm will be subjected to additional extrapharyngeal regulation in response to changes in the external environment. We note that the *mgl-1*-mediated inhibition of pharyngeal tone acts at the level of the intrinsic network activity, a situation that closely mimics when the worm is in an OFF-food state. Therefore, we designed the whole organism assay around comparisons of the worm pharyngeal pumping both on and off food. As we have described a shift in the tone of the pharyngeal pumping in whole worms kept for an increasing period of time off food (46), we conducted OFF-food measurements at 5 and 95 min. To this end, we used pharyngeal pumping in the presence of food and its response to food deprivation as a tractable way to probe for a functional correlation of the drug-mediated effect. We extended this to investigate wild-type animals and compared this to *mgl-1(tm1811)* animals. In addition, the single mutants *mgl-2(tm0355)* and *mgl-3(tm1766)* and the double mutant *mgl-1(tm1811);mgl-3(tm1766)* were included in the analysis to allow us to probe for functional evidence of the receptor interactions revealed in the semi-intact investigation of drug-mediated *mgl* activation. Although *mgl-2(tm0355)* did not display a phenotype in the LCCG-I EPG, the expression of *mgl-2* in the pharyngeal circuit suggests that it may modulate pharyngeal function, and therefore it was included in the analysis.

To investigate whether the MGL receptors are involved in the food-adaptive response, a paired analysis was performed on animals in the presence of food and after being deprived of food for a short and extended period of time. Pumping was counted for 1 min at four time points: 0 min, where the animal is in the presence of food, and 5 and 95 min after being transferred to a no-food environment. Worms were then returned to a food lawn, and the pharyngeal pumping rate was counted at 100 min (Fig. 8*A*).

The wild-type worms displayed context-dependent changes in the frequency of pharyngeal pumping. Initially, a high frequency of pumping was recorded in the presence of food (268.4 ± 3.7 S.E.). This decreased after 5 min off food and

underwent a time-dependent increase after being off food for 95 min. When placed back on food, the pumping rate increased toward the high pumping rate initially recorded on food. However, it did not recover completely (Fig. 8*B*). In the presence of food, the pumping rate of single and double *mgl* mutants was not significantly different from the wild type (Fig. 8*B*). After being food-deprived for 5 min, the pumping rate of wild-type animals on a no-food arena was reduced to 10.85 ± 3.23 (S.E.) pumps min^{-1} (Fig. 8*B*). After the same treatment, the pump rate of *mgl-1(tm1811)* was significantly higher than N2, 29.11 ± 6.09 pumps min^{-1} ($p < 0.05$). The pump rate of *mgl-2(tm0355)* was increased compared with N2 but not significantly different. The *mgl-3(tm1766)* pump rate was very similar from the wild type and not significantly different. This would suggest that *mgl-1* is active during processes that create the acute inhibition of pharyngeal pumping in response to food removal. The *mgl-3* mutants did not exhibit this loss of inhibitory tone. This observation is consistent with the EPG recordings made from *mgl-3* mutants, which suggest that this receptor subtype excites pharyngeal pumping in the presence of a low concentration of LCCG-I. In addition, the pump rate of the double mutant *mgl-1(tm1811);mgl-3(tm1766)* was not significantly different from the wild type after 5 min of food removal. This adds further support to the hypothesis that *mgl-1* and *mgl-3* activation has opposing effects on the activity of the pharyngeal nervous system, where *mgl-1* is inhibitory and *mgl-3* is excitatory. Following an extended period of food removal (95 min), the pharyngeal pumping rate of the wild type increased to 53.68 ± 8 pumps min^{-1} (Fig. 8*B*). All *mgl* mutants tested exhibited an increased pharyngeal pumping rate after 95 min relative to counts made at 5 min off food. None of the rates recorded were significantly different from the wild type. When wild-type worms were returned to food after being starved for 95 min, the pharyngeal pump rate increased, approaching that initially recorded on food. The recovery of the *mgl* mutant strains was not significantly different from the wild-type worms (Fig. 8*B*). The rate of *mgl-3(tm1766)* pumping and *mgl-1(tm1811);mgl-3(tm1766)* pumping was not significantly different from the wild-type on food at the beginning of the experiment, after 95 min off food and when returned to food.

The analysis of context-dependent behavior would suggest that the loss of *mgl-1* function has the greatest impact upon the acute response to food removal. To confirm the role of *mgl-1* in the acute response to food removal, the pumping rate of the rescue strain *mgl-1(tm1811);ZC506* was measured after 5 min of food removal and compared with *mgl-1(tm1811)* and wild-type strains (Fig. 8*C*). The rate of pumping of mgl-1 was significantly higher than N2, confirming the previous finding. The pumping rate of *mgl-1(tm1811)*;ZC506 was not significantly different from N2. This further supports the role for glutamate in the negative regulation of pharyngeal behavior in response to acute food removal in the whole worm. In addition, it highlights the contribution made by *mgl-1* in setting the inhibitory tone in response to changes in environmental sensory cues and the role of this receptor in modulating the activity of the pharyngeal neural network.

Discussion

The mgls: a Conserved Arm of Glutamatergic Transmission in C. elegans—Three receptors with the domain organization associated with mGluRs are annotated in Wormbase. Our characterization of the cDNAs was used to better define the coding sequence of the annotated genes. When the three *mgls* were compared, they showed as much homology to each other as they did to the most related mammalian mGluRs, arguing that they make up a family of receptors encompassing three distinct subtypes. This molecular organization therefore mirrors the situation that prevails in the vertebrate nervous system, where molecular ontogeny into groups I, II, and III is supported by selective pharmacological specificity and downstream signaling. The significance of this is that the identified molecular diversity of the *mgls* suggests that they have similar potential to diversify signaling output from glutamate transmission. It is particularly striking that proteins encoding these receptors have many of the motifs that impart functional regulation at the level of receptor phosphorylation and scaffolding that are known to further diversify the complexity of mGluR signaling (39).

Molecular Complexity to Extend Receptor Diversity—Performing 5′ and 3′ RACE on the predicted gene sequences allowed us to resolve apparently unappreciated complexity in the promoter elements and splice variants within coding sequences that can be derived from the gene locus of *mgl-1*, *mgl-2*, and *mgl-3*. In the case of gene control, our analysis provided more precise transcription start sites, many of which were authenticated by the presence of SL1 splice leader sequences. This is true for *mgl-1*, *mgl-2*, and *mgl-3*. In the latter case, the RACE revealed the existence of a large 5′ intron that interrupted an upstream non-coding exon in the 5′ end of the gene. This variant was amplified robustly but not preceded by a splice leader, and there is no intervening gene in this region. The amplification of a single transcript containing the open reading frame for both *mgl-2* and the transcription factor *maf-1* further highlights an apparent complexity of *mgl* function. The functional relevance of this finding is unclear. However, it exemplifies the wider theme that there is potential for selective elements to control the developmental, temporal, and spatial expression of the receptors.

Widespread and Complimentary Expression of mgls—We used available GFP reporter strains to visualize the expression of *mgl-1* and complemented this with constructs designed to look at *mgl-2* and *mgl-3* expression. These reporters encompass many key determinants of the likely promoter regions and should provide rather faithful expression, therefore suggesting that these receptors are restricted to the nervous system. Nevertheless the potential for further important expression beyond that documented by these reporters cannot be ruled out, particularly when, as in the *mgl-3* genes, there are clearly relatively complex promoter sequences. The expression patterns were relatively distinct, and all cases seemed restricted to the nervous system. *mgl-1*, *mgl-2*, and *mgl-3* were expressed in the nerve ring, and they were also expressed in tail neurons.

mgl-1, *mgl-2*, and *mgl-3* expression patterns appeared distinct, but there was an overlap in the case of the pharyngeal

nervous system. This represents a microcircuit of 20 neurons that release a mixture of fast transmitters and neuromodulators that regulate pharyngeal pumping. Striking in this was the clear overlapping expression of *mgl-1*, *mgl-2*, and *mgl-3* in NSM, the neurosecretory neuron that expresses the stimulatory modulator 5-HT. This expression suggested the potential coordinated use of these receptors in regulation of the pharynx. Although NSM is a classic neurosecretory 5-HT-releasing neuron, it additionally expresses the vesicular glutamate transporter, suggesting the potential to release glutamate (40) and other neuropeptide modulators (41). Although the expression of these *mgls* in a glutamate-releasing neuron would support a role as autoreceptors, the wide expression of *mgl-1* in particular highlights their potential to act as both pre- and postsynaptic detectors of glutamate. As detailed by comparison of ours (Fig. 3) and others (42, 43), the expression of *mgl-1* and *mgl-3* extends to a number of non-glutamatergic neurons, suggesting a broad potential in the regulation of the neuronal pharyngeal microcircuit.

Pharmacological Dissection of MGL Function—The expression of *mgl-1*, *mgl-2*, and *mgl-3* in the pharynx lent itself to the functional investigation of these receptors. None of the *mgl* mutants exhibited a discernible change in their pumping *per se* when measured using extrapharyngeal recording of the EPG. In contrast, activation with two distinct mGluR agonists known to activate invertebrate receptors (12, 14) produced a dose-dependent inhibition of pharyngeal function. Importantly, this major inhibitory effect was lost in the *mgl-1* mutants and suggests that these agonists lead to functionally coupled *mgl-1* receptor activation. LCCG-I effects were not impacted in the *mgl-2* mutant, suggesting that this receptor subtype does not contribute to the agonist-mediated inhibition of pharyngeal pumping. EPGs recorded from *mgl-1*, *mgl-2*, and *mgl-3* mutants, in response to a low concentration of LCCG-I suggests a cross-talk between *mgl-1* and *mgl-3*. This could arise through one cell because both receptors are expressed in NSM, where *mgl-1* could inhibit and *mgl-3* promotes stimulatory output of this cell. This could be readily achieved by each receptor having distinct downstream signaling despite their shared activation by a common agonist, glutamate. This situation is aped in the sensory pathway of the worm at the level of ionotropic receptor signaling (21). An alternative explanation could be that this effect relates to differential activation of cells that selectively express the receptors. A striking feature of the *mgl-1*-mediated LCCG-1 effects is that it leads to a complete but reversible inhibition of pharyngeal pumping. One might predict that, in a structure like the pharynx, which is myogenic (36), that it would be difficult to achieve this with an agonist that indirectly modulates the muscle by neurogenic control. The intracellular recordings did not identify a direct effect of the MGL agonist on the muscle consistent with an indirect effect. A rebound response was observed upon removal of the agonist during the washout period. Indeed, such a phenomenon has been identified as a physiologically relevant way of imparting control within important sensory pathways, including those that signal to higher function. In such scenarios, the reduction of agonist activity can act as a stimulation of network activity (44). Such a modulation may allow for excitatory signaling in a network because *mgl*-mediated inhibition is tonically changed in response to chronic changes in circulating glutamate. In the context of the pharynx, this could derive from synaptically released glutamate, but the pharyngeal neurons are well placed to sense changing concentrations of metabolites in the pseudocoelomic fluid. In this regard, it is interesting to note that chronic effects of *mgl-1* and *mgl-2* have been noted with respect to starvation responses (42). This, along with their conserved role as taste and gustatory receptors, opens up the potential of pharyngeal receptors to coordinate nutritional cues as well as participate through more classical synaptic activation.

In a reverberating circuit in which one assays network activity, it can be difficult to resolve the precise locus of receptor-mediated inhibition. Indeed, the widespread expression of *mgl-1* suggests a broad potential for receptor activation to act in glutamate-releasing/sensing neurons. This is borne out by our experiments in which we selectively activated the circuit by light stimulation of the glutamate-releasing neurons. This approach resolves a highly coupled muscle depolarization that involves a post-stimulation depolarization with a superimposed action potential. The initial event is largely dependent on glutamate but appears not to be selectively effected by LCCG-1-mediated *mgl-1* activation. In contrast, there is a more complete inhibition of the superimposed action potential that is driven by glutamate release onto the muscle and additional synaptically driven glutamate events that, in turn, drive cholinergic release in the pharyngeal microcircuits. This suggests that *mgl-1* could potentially act at several loci in the pharyngeal microcircuit, and cell-specific rescue of *mgl-1* function would be required to determine whether this is an evenly distributed network effect or whether it derives from a more discrete determinant.

Regulation of Pharyngeal Function and Beyond—The analysis of MGL function in the pharynx has the virtue of allowing a combination of mutants and pharmacological investigation of function. However, this preparation failed to resolve a clear difference in the wild-type and mutant pharynges with respect to their unstimulated pumping. For this reason, we tested the pharyngeal response in the intact animal with respect to distinct food stimulation.

However, as indicated in the pharmacological experiments, *mgl-1* activation produces a potent inhibition of pumping. Therefore, one might predict that this receptor mutant would display an exaggerated response to food. This simple view neglects the possibility that the pharyngeal nervous system is additionally providing an integrated control of the pharynx in the absence of food. This is reinforced by the observations in the sensory systems detailing an acute response to mimics of food removal (21). With this in mind, we investigated pharyngeal pumping on food and at two time points after removal from food. These data in the wild type recapitulate observations that suggest that, after food removal, worms stop pumping and slowly increase this for up to 90 min (45, 46). Observations that receptor activation by modulators and neuropeptides inhibits pumping and the data reported in this study suggest that the pharynx and its embedded microcircuit allows for an intricate balance in tone. Mutants that exhibit an exaggerated pumping in response to food withdrawal suggest that there is a loss of this tone. The observation that *mgl-1* mutants belong to this class

suggests that they function in such a way and is consistent with the observation that pharmacological activation of the receptor leads to an inhibition of pharyngeal function. The expression pattern of *mgl-1* and the tractable effect of mGluR agonists in the isolated pharyngeal preparations suggest that *mgl-1* could exert such an effect at the level of the circuit within the intact organism. The exaggerated pumping phenotype of *mgl-1(tm1811)* was restricted to early time points following acute food removal, and the elevated pumping after a prolonged period off food was equivalent in all mutant backgrounds. These observations highlight the selective contribution of *mgl-1* at a discrete time point of an adaptive response.

Overall, our observations highlight a powerful effect of *mgl-1* in the modulation of pharyngeal pumping behavior. The modulation revealed by pharmacological investigations is reinforced by behavioral investigations and suggest a wider significance of MGL-mediated signaling. As highlighted by the molecular diversity of *C. elegans* mgl subtypes, this mode of glutamate signaling already exhibits significant complexity. Therefore, *C. elegans* can model fundamental aspects of the key processes by which these receptors underpin function in higher organisms.

Acknowledgments—Some strains were provided by the CGC, which is funded by National Institutes of Health Office of Research Infrastructure Programs (P40 OD010440).

References

1. Watkins, J. C., Davies, J., Evans, R. H., Francis, A. A., and Jones, A. W. (1981) Pharmacology of receptors for excitatory amino acids. *Adv. Biochem. Psychopharmacol.* **27,** 263–273
2. Pin, J. P., and Duvoisin, R. (1995) The metabotropic glutamate receptors: structure and functions. *Neuropharmacology* **34,** 1–26
3. Awad, H., Hubert, G. W., Smith, Y., Levey, A. I., and Conn, P. J. (2000) Activation of metabotropic glutamate receptor 5 has direct excitatory effects and potentiates NMDA receptor currents in neurons of the subthalamic nucleus. *J. Neurosci.* **20,** 7871–7879
4. Heidinger, V., Manzerra, P., Wang, X. Q., Strasser, U., Yu, S. P., Choi, D. W., and Behrens, M. M. (2002) Metabotropic glutamate receptor 1-induced upregulation of NMDA receptor current: mediation through the Pyk2/Src-family kinase pathway in cortical neurons. *J. Neurosci.* **22,** 5452–5461
5. Herman, E. J., Bubser, M., Conn, P. J., and Jones, C. K. (2012) Metabotropic glutamate receptors for new treatments in schizophrenia. *Handb. Exp. Pharmacol.* **213,** 297–365
6. Oberman, L. M. (2012) mGluR antagonists and GABA agonists as novel pharmacological agents for the treatment of autism spectrum disorders. *Expert Opin. Investig. Drugs* **21,** 1819–1825
7. Yizhar, O., Fenno, L. E., Prigge, M., Schneider, F., Davidson, T. J., O'Shea, D. J., Sohal, V. S., Goshen, I., Finkelstein, J., Paz, J. T., Stehfest, K., Fudim, R., Ramakrishnan, C., Huguenard, J. R., Hegemann, P., and Deisseroth, K. (2011) Neocortical excitation/inhibition balance in information processing and social dysfunction. *Nature* **477,** 171–178
8. Rubenstein, J. L., and Merzenich, M. M. (2003) Model of autism: increased ratio of excitation/inhibition in key neural systems. *Genes Brain Behav.* **2,** 255–267
9. Kehrer, C., Maziashvili, N., Dugladze, T., and Gloveli, T. (2008) Altered excitatory-inhibitory balance in the NMDA-hypofunction model of schizophrenia. *Front. Mol. Neurosci.* **1,** 6
10. Conn, P. J., and Jones, C. K. (2009) Promise of mGluR2/3 activators in psychiatry. *Neuropsychopharmacology* **34,** 248–249
11. Brockie, P. J., and Maricq, A. V. (2006) Ionotropic glutamate receptors: genetics, behavior and electrophysiology. *WormBook*, 1–16
12. Parmentier, M. L., Pin, J. P., Bockaert, J., and Grau, Y. (1996) Cloning and functional expression of a *Drosophila* metabotropic glutamate receptor expressed in the embryonic CNS. *J. Neurosci.* **16,** 6687–6694
13. Krenz, W. D., Nguyen, D., Pérez-Acevedo, N. L., and Selverston, A. I. (2000) Group I, II, and III mGluR compounds affect rhythm generation in the gastric circuit of the crustacean stomatogastric ganglion. *J. Neurophysiol.* **83,** 1188–1201
14. Kucharski, R., Mitri, C., Grau, Y., and Maleszka, R. (2007) Characterization of a metabotropic glutamate receptor in the honeybee (*Apis mellifera*): implications for memory formation. *Invert. Neurosci.* **7,** 99–108
15. Washio, H. (2002) Glutamate receptors on the somata of dorsal unpaired median neurons in cockroach, *Periplaneta americana*, thoracic ganglia. *Zoolog. Sci.* **19,** 153–162
16. Weinshenker, D., Garriga, G., and Thomas, J. H. (1995) Genetic and pharmacological analysis of neurotransmitters controlling egg laying in *C. elegans*. *J. Neurosci.* **15,** 6975–6985
17. Wakabayashi, T., Kitagawa, I., and Shingai, R. (2004) Neurons regulating the duration of forward locomotion in *Caenorhabditis elegans*. *Neurosci. Res.* **50,** 103–111
18. Jorgensen, E. M. (2004) Dopamine: should I stay or should I go now? *Nat. Neurosci.* **7,** 1019–1021
19. Sawin, E. R., Ranganathan, R., and Horvitz, H. R. (2000) *C. elegans* locomotory rate is modulated by the environment through a dopaminergic pathway and by experience through a serotonergic pathway. *Neuron* **26,** 619–631
20. You, Y. J., Kim, J., Cobb, M., and Avery, L. (2006) Starvation activates MAP kinase through the muscarinic acetylcholine pathway in *Caenorhabditis elegans* pharynx. *Cell Metab.* **3,** 237–245
21. Chalasani, S. H., Chronis, N., Tsunozaki, M., Gray, J. M., Ramot, D., Goodman, M. B., and Bargmann, C. I. (2007) Dissecting a circuit for olfactory behaviour in *Caenorhabditis elegans*. *Nature* **450,** 63–70
22. Walker, D. S., Gower, N. J., Ly, S., Bradley, G. L., and Baylis, H. A. (2002) Regulated disruption of inositol 1,4,5-trisphosphate signaling in *Caenorhabditis elegans* reveals new functions in feeding and embryogenesis. *Mol. Biol. Cell* **13,** 1329–1337
23. Brenner, S. (1974) The genetics of *Caenorhabditis elegans*. *Genetics* **77,** 71–94
24. Flicek, P., Amode, M. R., Barrell, D., Beal, K., Brent, S., Chen, Y., Clapham, P., Coates, G., Fairley, S., Fitzgerald, S., Gordon, L., Hendrix, M., Hourlier, T., Johnson, N., Kähäri, A., Keefe, D., Keenan, S., Kinsella, R., Kokocinski, F., Kulesha, E., Larsson, P., Longden, I., McLaren, W., Overduin, B., Pritchard, B., Riat, H. S., Rios, D., Ritchie, G. R., Ruffier, M., Schuster, M., Sobral, D., Spudich, G., Tang, Y. A., Trevanion, S., Vandrovcova, J., Vilella, A. J., White, S., Wilder, S. P., Zadissa, A., Zamora, J., Aken, B. L., Birney, E., Cunningham, F., Dunham, I., Durbin, R., Fernández-Suarez, X. M., Herrero, J., Hubbard, T. J., Parker, A., Proctor, G., Vogel, J., and Searle, S. M. (2011) Ensembl 2011. *Nucleic Acids Res.* **39,** D800–806
25. Harris, T. W., Antoshechkin, I., Bieri, T., Blasiar, D., Chan, J., Chen, W. J., De La Cruz, N., Davis, P., Duesbury, M., Fang, R., Fernandes, J., Han, M., Kishore, R., Lee, R., Müller, H. M., Nakamura, C., Ozersky, P., Petcherski, A., Rangarajan, A., Rogers, A., Schindelman, G., Schwarz, E. M., Tuli, M. A., Van Auken, K., Wang, D., Wang, X., Williams, G., Yook, K., Durbin, R., Stein, L. D., Spieth, J., and Sternberg, P. W. (2010) WormBase: a comprehensive resource for nematode research. *Nucleic Acids Res.* **38,** D463–467
26. Altschul, S. F., Madden, T. L., Schäffer, A. A., Zhang, J., Zhang, Z., Miller, W., and Lipman, D. J. (1997) Gapped BLAST and PSI-BLAST: a new generation of protein database search programs. *Nucleic Acids Res.* **25,** 3389–3402
27. Edwards, R. J., Moran, N., Devocelle, M., Kiernan, A., Meade, G., Signac, W., Foy, M., Park, S. D., Dunne, E., Kenny, D., and Shields, D. C. (2007) Bioinformatic discovery of novel bioactive peptides. *Nat. Chem. Biol.* **3,** 108–112
28. Katoh, K., and Toh, H. (2008) Recent developments in the MAFFT multiple sequence alignment program. *Brief Bioinform.* **9,** 286–298
29. Price, M. N., Dehal, P. S., and Arkin, A. P. (2009) FastTree: computing large minimum evolution trees with profiles instead of a distance matrix.

Mol. Biol. Evol. **26,** 1641–1650
30. Mello, C., and Fire, A. (1995) DNA transformation. *Methods Cell Biol.* **48,** 451–482
31. Franks, C. J., Murray, C., Ogden, D., O'Connor, V., and Holden-Dye, L. (2009) A comparison of electrically evoked and channel rhodopsin-evoked postsynaptic potentials in the pharyngeal system of *Caenorhabditis elegans*. *Invert. Neurosci* **9,** 43–56
32. Dillon, J., Hopper, N. A., Holden-Dye, L., and O'Connor, V. (2006) Molecular characterization of the metabotropic glutamate receptor family in *Caenorhabditis elegans*. *Biochem. Soc. Trans.* **34,** 942–948
33. Tharmalingam, S., Burns, A. R., Roy, P. J., and Hampson, D. R. (2012) Orthosteric and allosteric drug binding sites in the *Caenorhabditis elegans* mgl-2 metabotropic glutamate receptor. *Neuropharmacology* **63,** 667–674
34. Mitri, C., Parmentier, M. L., Pin, J. P., Bockaert, J., and Grau, Y. (2004) Divergent evolution in metabotropic glutamate receptors: a new receptor activated by an endogenous ligand different from glutamate in insects. *J. Biol. Chem.* **279,** 9313–9320
35. Conn, P. J., and Pin, J. P. (1997) Pharmacology and functions of metabotropic glutamate receptors. *Annu. Rev. Pharmacol. Toxicol.* **37,** 205–237
36. Avery, L., and Horvitz, H. R. (1989) Pharyngeal pumping continues after laser killing of the pharyngeal nervous system of *C. elegans*. *Neuron* **3,** 473–485
37. Rogers, C. M., Franks, C. J., Walker, R. J., Burke, J. F., and Holden-Dye, L. (2001) Regulation of the pharynx of *Caenorhabditis elegans* by 5-HT, octopamine, and FMRFamide-like neuropeptides. *J. Neurobiol.* **49,** 235–244
38. Avery, L., and Horvitz, H. R. (1990) Effects of starvation and neuroactive drugs on feeding in *Caenorhabditis elegans*. *J. Exp. Zool.* **253,** 263–270
39. Enz, R. (2007) The trick of the tail: protein-protein interactions of metabotropic glutamate receptors. *BioEssays* **29,** 60–73
40. Lee, R. Y., Sawin, E. R., Chalfie, M., Horvitz, H. R., and Avery, L. (1999) EAT-4, a homolog of a mammalian sodium-dependent inorganic phosphate cotransporter, is necessary for glutamatergic neurotransmission in *Caenorhabditis elegans*. *J. Neurosci.* **19,** 159–167
41. Nathoo, A. N., Moeller, R. A., Westlund, B. A., and Hart, A. C. (2001) Identification of neuropeptide-like protein gene families in *Caenorhabditis elegans* and other species. *Proc. Natl. Acad. Sci. U.S.A.* **98,** 14000–14005
42. Kang, C., and Avery, L. (2009) Systemic regulation of starvation response in *Caenorhabditis elegans*. *Genes Dev.* **23,** 12–17
43. Greer, E. R., Pérez, C. L., Van Gilst, M. R., Lee, B. H., and Ashrafi, K. (2008) Neural and molecular dissection of a *C. elegans* sensory circuit that regulates fat and feeding. *Cell Metab.* **8,** 118–131
44. Zheng, N., and Raman, I. M. (2011) Prolonged postinhibitory rebound firing in the cerebellar nuclei mediated by group I metabotropic glutamate receptor potentiation of L-type calcium currents. *J. Neurosci.* **31,** 10283–10292
45. Avery, L., and You, Y. J. (2012) *C. elegans* feeding. *WormBook*, 1–23
46. Dalliere, N., Bhatla, N., Walker, R., O'Connor, V., and Holden-Dye, L. (2014) Neuronal Development, Synaptic Function, and Behavior *C. elegans* Topic Meeting, Madison, WI 2014 (Hart, A., ed) p. 66, Madison, WI
47. Ishihara, T., and Katsura, I. (1996) Worm Breeder's Gazette (Avery, L., ed) **14,** 40
48. Franks, C. J., Murray, C., Ogden, D., O'Connor, V., and Holden-Dye, L. (2010) European *C. elegans* Neurobiology Meeting, Fodele Village, 2010 (Tavernarakis, N., ed.) p. 40, P06, Crete, Greece